

Non-standard Hamiltonian effects on neutrino oscillations

MATTIAS BLENNOW^a, TOMMY OHLSSON^b, AND WALTER WINTER^c

^{a,b}*Department of Theoretical Physics, School of Engineering Sciences,
Royal Institute of Technology (KTH) – AlbaNova University Center,
Roslagstullsbacken 11, 106 91 Stockholm, Sweden*

^c*School of Natural Sciences, Institute for Advanced Study,
Einstein Drive, Princeton, NJ 08540, USA*

Abstract

We investigate non-standard Hamiltonian effects on neutrino oscillations which are effective additional contributions to the vacuum Hamiltonian similar to the Mikheyev–Smirnov–Wolfenstein matter potential. In this context, we develop a general framework for such effects with two neutrino flavors and discuss the extension to three neutrino flavors. The simplest of these effects are classified as either flavor or mass effects, which both can be conserving or violating (changing). In both flavor and mass bases, we derive the effective neutrino oscillation parameters due to these effects. In addition, we find that the resonance condition is modified for flavor conserving effects as well as for both mass conserving and violating effects. The non-standard Hamiltonian effects on the effective mixing and the two-flavor appearance probability are visualized and described in detail. Furthermore, we point out the difference of non-standard Hamiltonian effects from so-called “damping effects” on neutrino oscillations probabilities, which we have recently studied in another paper. Finally, we discuss experimental strategies how one could test and identify specific non-standard effects in future neutrino experiments, and we demonstrate the challenges for a neutrino factory with a numerical example.

^aEmail: mbl@theophys.kth.se

^bEmail: tommy@theophys.kth.se

^cEmail: winter@ias.edu

1 Introduction

Neutrino physics has entered the era of precision measurements of the fundamental neutrino parameters such as neutrino mass squared differences and leptonic mixing parameters, and neutrino oscillations are the most credible candidate for describing neutrino flavor transitions. Nevertheless, there might be other sub-leading mechanisms participating in the total description of neutrino flavor transitions. Thus, in this paper, we will investigate such mechanisms on a fundamental level, which will give rise to non-standard effects on the ordinary framework of neutrino oscillations.

In a previous paper [1], we have studied non-standard effects on probability level based on “damping signatures”, which were phenomenologically introduced in the neutrino oscillation probabilities. However, in this paper, we will investigate so-called non-standard Hamiltonian effects, which are effects on Hamiltonian level rather than on probability level. Recently, three different main categories of non-standard Hamiltonian effects have been discussed in the literature. These categories are non-standard interactions (NSI), flavor changing neutral currents (FCNC), and mass varying neutrinos (MVN or MaVaNs). Below, we will shortly review these categories of effects.

In general, in many models, neutrino masses come together with NSI, which means that the evolution of neutrinos passing through matter is modified by non-standard potentials due to coherent forward-scattering of NSI processes $\nu_\alpha + f \rightarrow \nu_\beta + f$, where $\alpha, \beta = e, \mu, \tau$ and f is a fermion in matter.¹ The effective NSI potentials are given by $V_{\text{NSI}} = \sqrt{2}G_F N_d \epsilon_{\alpha\beta}$, where G_F is the Fermi coupling constant, N_d is the down quark number density, and $\epsilon_{\alpha\beta}$ ’s are small parameters describing the NSI [2]. See, *e.g.*, Ref. [3] for a recent review. Furthermore, matter-enhanced neutrino oscillations in presence of Z -induced FCNC have been studied in the literature [4–6]. See also, *e.g.*, Refs. [7, 8] for some earlier contributions. Especially, NSI and FCNC have been investigated in several references for many different scenarios such as for solar [9–12], atmospheric [13–17], supernova [18], and other astrophysical neutrinos as well as for CP -violation [19], the LSND experiment [20], beam experiments [21], and neutrino factories [22–27].

The idea of MVN was proposed by Fardon *et al.* in Refs. [28, 29]. This idea is based on the dark energy of the Universe being neutrinos which can act as a negative pressure fluid and be the origin of cosmic acceleration. Furthermore, several continuation works on MVN have been performed in the context of scenarios for the Sun and the solar neutrino deficit [30, 31], but also in various other contexts [32–43]. In addition, it should be mentioned that neutrinos with variable masses have also been studied earlier than the idea of MVN [28, 44–47].

The paper is organized as follows: First, in Sec. 2, we define non-standard Hamiltonian effects as effective additional contributions to the vacuum Hamiltonian similar to matter effects. The definition is performed for n neutrino flavors. Next, in Sec. 3, we specialize our discussion to two neutrino flavors. Furthermore, we set the stage with a general formalism and derive the effective neutrino parameters as well as the resonance conditions in both flavor and mass bases including non-standard Hamiltonian effects. At the end of this section, we visualize the non-standard effects on the effective mixing. Next, in Sec. 4, we study

¹Note that, in general, the production and detection vertices could also be modified.

some aspects of the generalization to three-flavor oscillations. Then, in Sec. 5, we discuss general experimental strategies to test and identify non-standard Hamiltonian effects, while in Sec. 6, we give a numerical example of how non-standard Hamiltonian effects can affect a realistic experimental setup. Finally, in Sec. 7, we summarize our results and present our conclusions.

2 Non-standard Hamiltonian effects

In the standard neutrino oscillation framework with n flavors, the Hamiltonian in vacuum is given by

$$H = \frac{1}{2E} U \text{diag}(m_1^2, m_2^2, \dots, m_n^2) U^\dagger \quad (1)$$

in flavor basis, where E is the neutrino energy, U is the leptonic mixing matrix, and m_i is the mass of the i th neutrino mass eigenstate. Any Hermitian non-standard Hamiltonian effect will alter this vacuum Hamiltonian into an effective Hamiltonian

$$H_{\text{eff}} = H + H', \quad (2)$$

where H' is the effective contribution to the vacuum Hamiltonian. We note that this reminds of neutrino mixing and oscillations in matter [7] with H' given by a diagonal matrix with the effective matter potentials on the diagonal, *i.e.*,

$$H' = H_{\text{mat}} = \text{diag}(V, 0, \dots, 0) - \frac{1}{\sqrt{2}} G_F N_n \mathbf{1}_n, \quad (3)$$

where $V = \sqrt{2} G_F N_e$ is the ordinary matter potential, G_F is the Fermi coupling constant, N_e is the electron number density (resulting from coherent forward-scattering of neutrinos), N_n is the nucleon number density, and $\mathbf{1}_n$ is the $n \times n$ unit matrix. Just as the presence of matter affects the effective neutrino mixing parameters, the effective neutrino mixing parameters will be affected by any non-standard Hamiltonian effect.

Since any part of the effective Hamiltonian that is proportional to the $n \times n$ unit matrix only contributes with an overall phase to the final neutrino state, it will not affect the neutrino oscillation probabilities. This means that we may assume H' to be traceless and also that we may subtract $\text{tr}(H)/n$ from the effective Hamiltonian to make it traceless. Any traceless Hermitian $n \times n$ matrix A may be written as

$$A = \sum_{i=1}^N c_i \lambda_i, \quad (4)$$

where the c_i 's are real numbers, the λ_i 's are the generators of the $su(n)$ Lie algebra (*i.e.*, A is an element of the Lie algebra), and $N = n^2 - 1$ is the number of generators. Hence, clearly, any non-standard Hamiltonian effect H' is parameterized by the $n^2 - 1$ numbers c_i . In summary, we choose the coefficients of the generators of the $su(n)$ Lie algebra to parameterize any non-standard Hamiltonian effect.

In any basis (*e.g.*, flavor or mass basis), we may introduce $su(n)$ generators λ_i such that $n(n - 1)/2$ generators are off-diagonal with only two real non-zero entries, $n(n - 1)/2$

generators are off-diagonal with only two imaginary non-zero entries, and $n - 1$ generators are diagonal with real entries. For example, in the case of $n = 2$, we have the Pauli matrices

$$\lambda_1 = \sigma_1 = \begin{pmatrix} 0 & 1 \\ 1 & 0 \end{pmatrix}, \quad \lambda_2 = \sigma_2 = \begin{pmatrix} 0 & -i \\ i & 0 \end{pmatrix}, \quad \lambda_3 = \sigma_3 = \begin{pmatrix} 1 & 0 \\ 0 & -1 \end{pmatrix}. \quad (5)$$

We will denote the set of generators which are of the form λ_i in flavor basis by ρ_i and the set of generators which are of this form in mass basis by τ_i . Clearly, in flavor basis, we have the relations

$$\rho_i = \lambda_i \quad \text{and} \quad \tau_i = U \lambda_i U^\dagger, \quad (6)$$

where, in the case of two neutrino flavors,

$$U = \begin{pmatrix} \cos(\theta) & \sin(\theta) \\ -\sin(\theta) & \cos(\theta) \end{pmatrix}$$

is the two-flavor leptonic mixing matrix and θ is the corresponding mixing angle (when treating the three-flavor case, we will use the standard parameterization of the leptonic mixing with three mixing angles θ_{12} , θ_{23} , θ_{13} , and one CP -violating phase δ_{CP}). This implies that ρ_i and τ_i would be equal if there was no mixing in the leptonic sector. Furthermore, it is obvious that the matrices ρ_i can be written as linear combinations of the matrices τ_i and vice versa. Therefore, there is, in principle, no difference between effects added in flavor or mass basis, at least if one allows for the most general form of the non-standard contribution.

We now define any non-standard effect as a “pure” flavor or mass effect if the corresponding effective contribution to the Hamiltonian is given by

$$H' = c \rho_i \quad \text{or} \quad H' = c \tau_i, \quad (i \text{ fixed}) \quad (7)$$

respectively, where $c \in \mathbb{R}$. This means that we do not allow the most general form of a non-standard contribution. For simplicity, we will assume c to be a constant, which may not hold in general (it can be a function of the energy, matter density, *etc.*). This choice implies that only one of the generators is present, since a general linear combination, such as Eq. (4), can always be interpreted in both bases. Thus, we define a flavor or mass conserving (violating) effect as any effect where the effective contribution to the Hamiltonian is diagonal (off-diagonal) in the corresponding basis.² We note that a pure flavor (mass) violating effect corresponds to some interaction between two flavor (mass) eigenstates. For example, the $su(2)$ generators ρ_1 and ρ_2 correspond to flavor violating (or changing) effects, whereas ρ_3 corresponds to flavor conserving effects. In summary, if we detect an arbitrary non-standard effect, it is the simple form in flavor or mass basis which makes it a flavor or mass effect by our definition. This approach can be justified by the fact that the simplest models for non-standard effects correspond to specific patterns for the effective addition to the Hamiltonian. For instance, for MVN, a contribution diagonal in mass space is assumed. Therefore, our definition of a “pure effect” is a conceptually new one and it refers to a class of effects, which can be interpreted in different ways. However, since simplicity is a basic concept of physics, this concept allows the choice of the most “natural” non-standard effects for further testing.

²Strictly speaking, our definition distinguishes (in two-flavors) off-diagonal additions proportional to λ_1 (real) or λ_2 (complex).

The case of non-standard Hamiltonian effects on three-flavor neutrino oscillations, *i.e.*, the case of $n = 3$, is quite similar to the one described above for the two-flavor case. Instead of the Pauli matrices, which are a basis of the $su(2)$ Lie algebra, we now have to use the eight Gell-Mann matrices, which span the $su(3)$ Lie algebra. Out of the Gell-Mann matrices, three are off-diagonal with real entries, three are off-diagonal with imaginary entries, and two are diagonal with real entries. Even though the principle of the three-flavor case is the same as that of the two-flavor case, it introduces many more parameters (more leptonic mixing angles, the complex phase in the leptonic mixing matrix, the extra mass squared difference, and the extra degrees of freedom for the non-standard effects), and therefore, turns out to be much more cumbersome to handle than the two-flavor case. In the following, we will mainly focus on the two-flavor case.

As far as the classification of current models in our notation is concerned, NSI and FCNC will be flavor effects, whereas MVN will be mass effects. In general, NSI can be of two types: flavor changing (FC) and non-universal (NU) [3]. The off-diagonal elements of the effective NSI potential $\epsilon_{\alpha\beta}$, where $\alpha \neq \beta$, correspond to FC, whereas the differences in the diagonal elements $\epsilon_{\alpha\alpha}$ correspond to NU. In addition, FCNC are flavor violating effects and MVN are mass conserving effects. In principle, for our purposes, there is no difference between FC NSI and FCNC.

3 Non-standard Hamiltonian effects with two flavors

In this section, we will first derive a general formalism for non-standard Hamiltonian effects with two flavors. Then, we will specialize our derivation to two bases, flavor and mass basis, which are obviously linearly dependent, but should be the canonical way to continue our discussion.

3.1 General formalism

As discussed above, any two-flavor Hamiltonian can be written in flavor basis on the form

$$H = \mathbf{H} \cdot \boldsymbol{\sigma}, \quad (8)$$

where $\mathbf{H} \in \mathbb{R}^3$ and $\boldsymbol{\sigma} = (\sigma_1, \sigma_2, \sigma_3)$ is the vector of the three Pauli matrices (*cf.*, the pictorial description of two-flavor neutrino oscillations in Ref. [48]). For a time-independent Hamiltonian, the time evolution operator is given by

$$S(t) = \exp(-iHt). \quad (9)$$

Using the relation $(\mathbf{A} \cdot \boldsymbol{\sigma})^2 = |\mathbf{A}|^2$, one obtains

$$S(t) = \mathbf{1}_2 \cos(|\mathbf{H}|t) - i \frac{H}{|\mathbf{H}|} \sin(|\mathbf{H}|t), \quad (10)$$

where $\mathbf{1}_2$ is the 2×2 unit matrix. This gives the two-flavor neutrino oscillation probabilities of the form

$$P_{\alpha\alpha} = \text{tr}[P_+ S(t)] = 1 - \sin^2(2\tilde{\theta}) \sin^2(kt), \quad (11)$$

$$P_{\alpha\beta} = \text{tr}[P_- S(t)] = \sin^2(2\tilde{\theta}) \sin^2(kt), \quad (12)$$

where

$$P_{\pm} = \frac{1 \pm \sigma_3}{2}, \quad \sin^2(2\tilde{\theta}) = \frac{H_1^2 + H_2^2}{|\mathbf{H}|^2}, \quad \text{and} \quad k = |\mathbf{H}| = \sqrt{\sum_{i=1}^3 H_i^2}.$$

Here the H_i 's are the components of the Hamiltonian and $\tilde{\theta}$ is the effective mixing angle.

In the standard two-flavor neutrino oscillation scenario, $H_1 = \sin(2\theta)\Delta m^2/(4E)$, $H_2 = 0$, and $H_3 = V/2 - \cos(2\theta)\Delta m^2/(4E)$. In general, the resonance condition, *i.e.*, the condition for maximal effective mixing, is $H_3 = 0$. The Hamiltonian is represented as a vector in \mathbb{R}^3 , the third direction being the “flavor” eigendirection. The mixing is given by the angle between the Hamiltonian vector and the flavor eigendirection. The mixing is maximal, *i.e.*, $\sin^2(2\tilde{\theta}) = 1$, when the Hamiltonian vector is orthogonal to the flavor eigendirection, which, as expected, is equivalent to the resonance condition.

The flavor and mass bases, and thus, the flavor and mass effects, are intimately associated with each other. For the case of $n = 2$, *i.e.*, for two neutrino flavors, any effective contribution to the Hamiltonian can be written in either flavor or mass basis, *i.e.*, as $H' = F_1\rho_1 + F_2\rho_2 + F_3\rho_3$ or $H' = M_1\tau_1 + M_2\tau_2 + M_3\tau_3$. Since the effect must be the same regardless of the basis it is expressed in, we obtain the relations

$$\begin{cases} F_1 = M_1 \cos(2\theta) - M_3 \sin(2\theta) \\ F_2 = M_2 \\ F_3 = M_1 \sin(2\theta) + M_3 \cos(2\theta) \end{cases} \quad (13)$$

from Eq. (6), *i.e.*, one obtains F_1 and F_3 by rotating M_1 and M_3 by the angle -2θ as well as one has $F_2 = M_2$. Thus, the transformation in Eq. (13) relates flavor and mass effects and shows that they are linear combinations of each other. Next, we will discuss both the flavor and mass effects in detail.

3.2 Flavor effects

First, we discuss flavor effects which are effects proportional to ρ_i . In this case, flavor conserving effects will be contributions to the total Hamiltonian on the form $H' = F_3\rho_3$, where $F_3 \in \mathbb{R}$, whereas flavor violating effects will be contributions on the form $H' = F_1\rho_1 + F_2\rho_2$, where $F_i \in \mathbb{R}$. Thus, in flavor basis, the new effective parameters are given by

$$\Delta\tilde{m}^2 = \Delta m^2\xi, \quad (14)$$

$$\sin^2(2\tilde{\theta}) = \frac{\left[\frac{4EF_1}{\Delta m^2} + \sin(2\theta)\right]^2 + \left(\frac{4EF_2}{\Delta m^2}\right)^2}{\xi^2}, \quad (15)$$

where

$$\xi = \sqrt{\left[\frac{4EF_1}{\Delta m^2} + \sin(2\theta)\right]^2 + \left(\frac{4EF_2}{\Delta m^2}\right)^2 + \left[\frac{2VE}{\Delta m^2} + \frac{4EF_3}{\Delta m^2} - \cos(2\theta)\right]^2} \quad (16)$$

is the normalized length of the Hamiltonian vector, $\Delta\tilde{m}^2$ is the effective mass squared difference in flavor basis, and $\tilde{\theta}$ is the effective mixing angle in flavor basis.³ In addition,

³Note that F_2 may also change the effective Majorana phase.

the resonance condition is found to be

$$\frac{2VE}{\Delta m^2} + \frac{4EF_3}{\Delta m^2} = \cos(2\theta), \quad (17)$$

which is clearly nothing but a somewhat modified version of the Mikheyev–Smirnov–Wolfenstein (MSW) resonance condition [7, 49, 50]. From the resonance condition in Eq. (17), it is easy to observe that the resonance is present for some energy E if and only if

$$\operatorname{sgn}(\Delta m^2) \operatorname{sgn}(V) \operatorname{sgn}(1 + 2F_3/V) = 1, \quad (18)$$

where $\operatorname{sgn}(\Delta m^2)$ is dependent on the mass hierarchy, $\operatorname{sgn}(V)$ is dependent on if we are studying neutrinos or anti-neutrinos, and $\operatorname{sgn}(1 + 2F_3/V)$ is dependent on the ratio between F_3 and the matter potential V [$\operatorname{sgn}(1 + 2F_3/V)$ being equal to -1 if and only if F_3 has a magnitude larger than $|V/2|$ and is of opposite sign to V]. Note that if there are flavor violating contributions added to the Hamiltonian, then these do not change the resonance condition. This can be easily understood, since the effective contribution to the Hamiltonian from any flavor violating effect will be parallel to the $H_3 = 0$ plane.

The series expansions to first of order of the effective mixing angle and the normalized length of the Hamiltonian vector in flavor basis are found to be

$$\sin(2\tilde{\theta}) \simeq \frac{\sin(2\theta)}{\xi_0} + \frac{4EQ}{\Delta m^2 \xi_0^3} [F_1 Q + F_3 \sin(2\theta)], \quad (19)$$

$$\xi \simeq \xi_0 + \frac{4E}{\Delta m^2 \xi_0} [F_1 \sin(2\theta) - F_3 Q], \quad (20)$$

where we have defined

$$\xi_0 = \sqrt{\sin^2(2\theta) + Q^2},$$

$$Q = \cos(2\theta) - \frac{2VE}{\Delta m^2}.$$

Note that flavor conserving effects enter only at second order at the matter resonance ($Q = 0$). This is due to the fact that the change in the Hamiltonian vector for a flavor conserving effect is then orthogonal to the Hamiltonian vector itself. At the matter resonance, the change of $\sin(2\tilde{\theta})$ due to any effect is of second order. This can be understood from the fact that this is an extremal point for $\sin(2\tilde{\theta})$, and thus, the derivative with respect to any component of the Hamiltonian vector must be equal to zero. The reason why F_2 enters only at second order is that this always indicates a change in the Hamiltonian vector which is orthogonal to the original Hamiltonian vector.

3.3 Mass effects

Second, we discuss mass effects which are effects proportional to τ_i , *i.e.*, effects proportional to $U\sigma_i U^\dagger$ in flavor basis. In analogy with the flavor effects, mass conserving effects will be contributions to the total Hamiltonian on the form $H' = M_3\tau_3$, where $M_3 \in \mathbb{R}$, whereas

mass violating effects will be contributions on the form $H' = M_1\tau_1 + M_2\tau_2$, where $M_i \in \mathbb{R}$. Thus, in mass basis, the new effective parameters are given by

$$\Delta\tilde{m}^2 = \Delta m^2\xi, \quad (21)$$

$$\sin^2(2\tilde{\theta}) = \frac{\left[\frac{4EM_1}{\Delta m^2}\cos(2\theta) + \left(1 - \frac{4EM_3}{\Delta m^2}\right)\sin(2\theta)\right]^2 + \left(\frac{4EM_2}{\Delta m^2}\right)^2}{\xi^2}, \quad (22)$$

where

$$\xi = \sqrt{\left[\frac{2VE}{\Delta m^2}\sin(2\theta) + \frac{4EM_1}{\Delta m^2}\right]^2 + \left(\frac{4EM_2}{\Delta m^2}\right)^2 + \left[\frac{2VE}{\Delta m^2}\cos(2\theta) + \frac{4EM_3}{\Delta m^2} - 1\right]^2}. \quad (23)$$

In this case, the resonance condition is

$$\frac{2VE}{\Delta m^2} + \frac{4EM_1}{\Delta m^2}\sin(2\theta) + \frac{4EM_3}{\Delta m^2}\cos(2\theta) = \cos(2\theta). \quad (24)$$

Note that both mass conserving effects and mass violating effects enter into the resonance condition, whereas only the flavor conserving effects entered in the corresponding expression in the flavor basis [*cf.*, Eq. (17)]. This is due to the fact that the changes of the Hamiltonian vector from such effects are not parallel to the $H_3 = 0$ plane (in flavor basis). However, M_2 does not enter into the resonance condition, since $\sigma_2 = \tau_2$, *i.e.*, the change of the Hamiltonian vector is parallel to $H_3 = 0$ for such an effect.

Again, the series expansions to first order of the effective mixing angle and the normalized length of the Hamiltonian vector in mass basis are found to be

$$\sin(2\tilde{\theta}) \simeq \frac{\sin(2\theta)}{\xi_0} + \frac{4EQ}{\Delta m^2\xi_0^3} \left[M_1Q' + M_3\frac{2EV}{\Delta m^2}\sin(2\theta) \right], \quad (25)$$

$$\xi \simeq \xi_0 + \frac{4E}{\Delta m^2\xi_0} \left[M_1\frac{2VE}{\Delta m^2}\sin(2\theta) - M_3Q' \right], \quad (26)$$

where we have defined

$$Q' = 1 - \frac{2VE}{\Delta m^2}\cos(2\theta).$$

Note that $F_2 = M_2$ enters only at second order in all expressions. The reason was discussed in the flavor case. Both M_1 and M_3 enter at first order for ξ at the resonance, the corresponding changes in the Hamiltonian vector are not orthogonal to the Hamiltonian vector itself. However, at $Q' = 0$, the change corresponding to M_3 is orthogonal to the Hamiltonian vector. If matter effects are not included, *i.e.*, if the matter potential $V = 0$, then a non-zero M_1 enters only at second order. The reason for this is that the corresponding change in the Hamiltonian vector is orthogonal to the Hamiltonian vector itself. Again, at the resonance ($Q = 0$), all effects in $\sin(2\tilde{\theta})$ enter only at second order for the same reasons as stated in the flavor case. The change in $\sin(2\tilde{\theta})$ at $V = 0$ is not dependent on M_3 , since this corresponds to a change of the Hamiltonian vector parallel to itself. For the same reason, $\sin(2\tilde{\theta})$ is not sensitive to M_1 at $Q' = 0$.

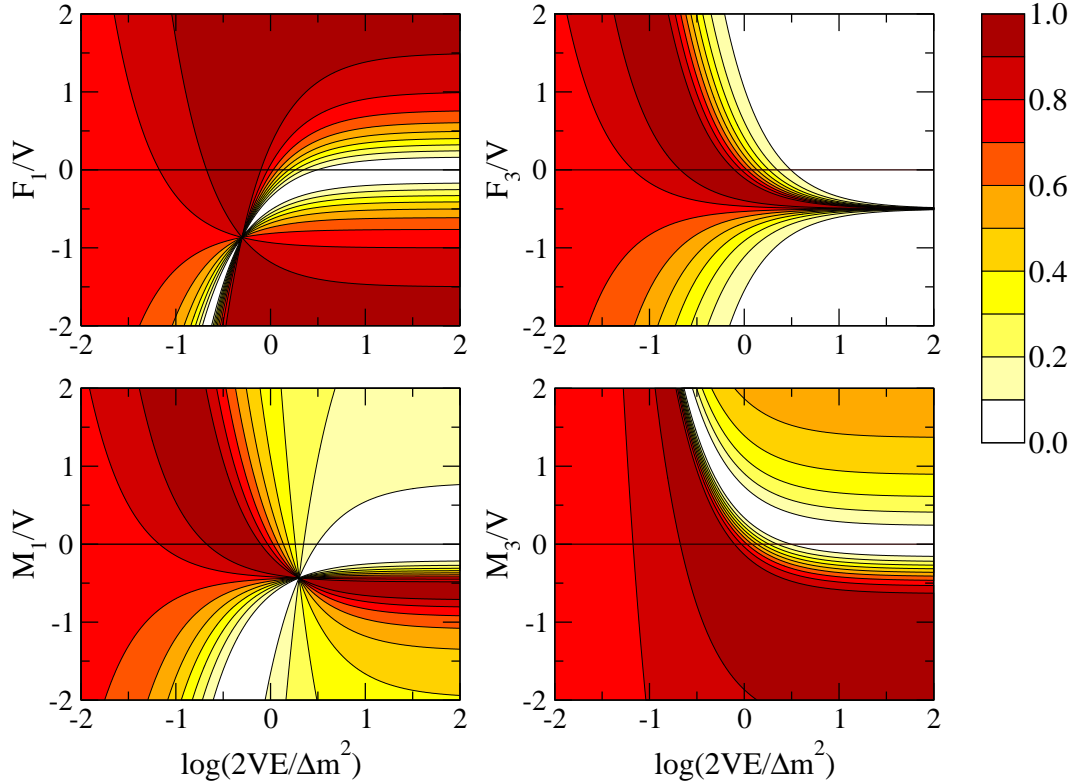


Figure 1: The effective mixing $\sin^2(2\tilde{\theta})$ as a function of $2VE/\Delta m^2$ and the ratio between the pure flavor (F_1 and F_3) or mass (M_1 and M_3) effects and the matter potential V . The horizontal lines correspond to no non-standard effect and the mixing along them is therefore the same in all panels. The vacuum mixing is assumed to be $\theta = 30^\circ$, which is close to the present value of the solar mixing angle θ_{12} (see, *e.g.*, Ref. [51]). See the main text for a more detailed discussion.

3.4 Visualization of non-standard effects on the effective mixing

It can be interesting (and quite illuminating) to study how different pure (flavor or mass) effects affect the effective neutrino mixing and oscillations. In this section, we assume that the non-standard effects are pure and have no energy dependence, *i.e.*, they behave in a fashion similar to the matter potential. In Fig. 1, we plot these pure flavor and mass effects. From this figure, some features become quite apparent, *e.g.*, some generic features are the shift in the resonance energy for F_3 , M_1 , and M_3 , the non-zero high-energy mixing for all effects but the flavor conserving effect F_3 , and the appearance of an anti-resonance – where $\sin^2(2\tilde{\theta})$ goes to zero for some finite energy – for F_1 , M_1 , and M_3 .

The shift in the resonance energy is simply due to the shift in the H_3 -component of the total effective Hamiltonian in flavor basis (as was mentioned earlier, the resonance condition is $H_3 = 0$). The fact that there is no shift of the resonance condition for F_1 and F_2 was also discussed earlier.

The reason why the effective high-energy mixing turns out to be non-zero is also quite easy

to realize. At high energies, the effective matter potential, which is diagonal in flavor basis, dominates over the vacuum Hamiltonian. As a result, the effective mixing is usually zero at high energies. However, if there is a non-standard effect with a corresponding effective addition to the Hamiltonian which is non-diagonal and scales with energy in the same way as the matter potential, then the effective mixing at high energies will be fully determined by the ratio of the non-standard effect and the matter potential.

The anti-resonance appears when $H_1 = H_2 = 0$ in flavor basis. Since $H_2 = 0$ in the standard neutrino oscillation scenario, it is apparent that this anti-resonance will occur for some value of F_1 . In addition, since M_1 and M_3 are linear combinations of F_1 and F_3 , the anti-resonance will also appear for M_1 and M_3 effects, as can be seen from the plots in Fig. 1.

There are also some interesting features that are specific for different effects. First, for F_1 effects, we note that the resonance condition is unchanged and that the mixing is constant as a function of energy for $F_1/V = -\tan(2\theta)/2$ (the reason for this is that the sum of the non-standard Hamiltonian and the matter potential is proportional to the vacuum Hamiltonian). Then, for flavor conserving F_3 effects, we note that these correspond to changes in the effective matter potential. For $F_3/V < -1/2$, we obtain an effective matter potential which is negative, resulting in a disappearance of the resonance. Next, for M_1 effects, the mixing is constant when $M_1/V = -\sin(2\theta)/2$, in analogy with the F_1 effects (again, the reason is that the sum of the non-standard Hamiltonian and the matter potential is proportional to the vacuum Hamiltonian). Also in analogy with the F_1 effects is that there is a value of $2VE/\Delta m^2$, where the mixing does not depend on the M_1/V ratio. However, in the case of M_1 effects, this is not the resonance mixing, but rather a mixing of $\sin^2(2\tilde{\theta}) = \cos^2(2\theta)$, which appears at $2VE/\Delta m^2 = 1/\cos(2\theta)$. Finally, for mass conserving M_3 effects, we note that the resonance disappears when $2\cos(2\theta)M_3/V < -1$.

The reason why the equivalent F_2 and M_2 effects are not included is that these effects always lead to an increase in the effective mixing angle for all energies, and thus, those plots do not show as many interesting features as the plots included. In addition, we note that if the non-standard effects are energy dependent, then the effective mixing will be given by the mixing along some non-constant function of $2VE/\Delta m^2$ in Fig. 1.

4 Three-flavor effects

As was stated in the Sec. 2, the general three-flavor case is quite complicated. However, if we assume that the non-standard effects are small, then we can use perturbation theory to derive expressions for the change in the neutrino oscillation parameters. For example, the elements of the effective mixing matrix are given by

$$\tilde{U}_{\alpha i} = \langle \nu_\alpha | \tilde{\nu}_i \rangle, \quad (27)$$

where $|\tilde{\nu}_i\rangle$ is the eigenstate of the full Hamiltonian. To first order in perturbation theory, we have

$$|\tilde{\nu}_i\rangle = |\nu_i\rangle + \sum_{j \neq i} \frac{\langle \nu_j | H' | \nu_i \rangle}{E_i - E_j} |\nu_j\rangle = |\nu_i\rangle + 2E \sum_{j \neq i} \frac{H'_{ji}}{\Delta m_{ji}^2} |\nu_j\rangle, \quad (28)$$

and thus, we find

$$\tilde{U}_{\alpha i} = U_{\alpha i} + 2E \sum_{j \neq i} \frac{H'_{ji}}{\Delta m_{ji}^2} U_{\alpha j} \quad (29)$$

or, in terms of the non-standard addition given in flavor basis,

$$\tilde{U}_{\alpha i} = U_{\alpha i} + 2E \sum_{j \neq i} \sum_{\beta, \gamma} \frac{U_{\beta j} U_{\gamma i}^* H'_{\beta \gamma}}{\Delta m_{ji}^2} U_{\alpha j}. \quad (30)$$

We note that this approach is valid only if $|2E H'_{ij} / \Delta m_{ji}^2| \ll 1$. If this is not valid, then we have to use degenerate perturbation theory in order to obtain valid results.

As was discussed in Ref. [26], if θ_{13} is small enough, then non-standard interactions may mimic the effects of a larger θ_{13} (this can also be the case for other effects which are not usually treated along with neutrino oscillations, such as damping effects [1]). With the perturbation theory approach described above, this becomes very transparent. In any experimental setup, the value of the mixing angle θ_{13} is determined by the modulus of the element U_{e3} of the neutrino mixing matrix U . If we include non-standard effects, then the effective counterpart of this element is given by

$$\begin{aligned} \tilde{U}_{e3} = & U_{e3} + \frac{2E}{\Delta m_{31}^2} (1 + \alpha s_{12}^2) (s_{23} H'_{e\mu} + c_{23} H'_{e\tau}) + \\ & \alpha \frac{2E}{\Delta m_{31}^2} s_{12} c_{12} \left[c_{23}^2 H'_{\mu\tau} - s_{23}^2 H'_{\tau\mu} + \frac{1}{2} \sin(2\theta_{23}) (H'_{\mu\mu} - H'_{\tau\tau}) \right], \end{aligned} \quad (31)$$

where we have made a series expansion to first order in $\alpha = \Delta m_{21}^2 / \Delta m_{31}^2 \simeq 0.03$ and disregarded terms of second order in both H' and θ_{13} .

If U_{e3} is smaller than or of equal size to the other terms in this expression, then the θ_{13} determined by an experiment will not be the actual θ_{13} unless the non-standard effects are taken into account. It is worth to notice that if $\theta_{23} = 45^\circ$, then $c_{23} = s_{23}$ and only the imaginary part of $H'_{\mu\tau} = (H'_{\tau\mu})^*$ will enter into the expression for \tilde{U}_{e3} , indicating that if the leading term is the one containing $H'_{\mu\tau}$, then the effective CP -violating phase will be $\pm 90^\circ$.

Another interesting observation is that even if there are no non-standard effects, there is a term proportional to $\Delta V \equiv H'_{\mu\mu} - H'_{\tau\tau}$ in this expression. Because of the different matter potentials for ν_μ and ν_τ due to loop-level effects, this quantity will be of the order $\Delta V \simeq 10^{-5} V$.

In Fig. 2, we plot the possible range of $|\tilde{U}_{e3}|$ as a function of $\epsilon_{\max} V E$, where $H'_{\alpha\beta} = \epsilon_{\alpha\beta} V$, V is the matter potential, and $|\epsilon_{\alpha\beta}| < \epsilon_{\max}$. For comparison, a neutrino factory with a neutrino energy of $E = 50$ GeV and a matter density of 3 g/cm 3 will have $VE \simeq 6 \cdot 10^{-15}$ MeV 2 and the position at which we need to consider the possible range of $|\tilde{U}_{e3}|$ then depends on the bounds on the non-standard interaction parameters $\epsilon_{\alpha\beta}$. In general, the bounds for $\epsilon_{\alpha\beta}$ depend on the types of interactions that are considered. It is common to write the non-standard interaction parameters as

$$\epsilon_{\alpha\beta} = \sum_f \epsilon_{\alpha\beta}^f \frac{N_f}{N_e}, \quad (32)$$

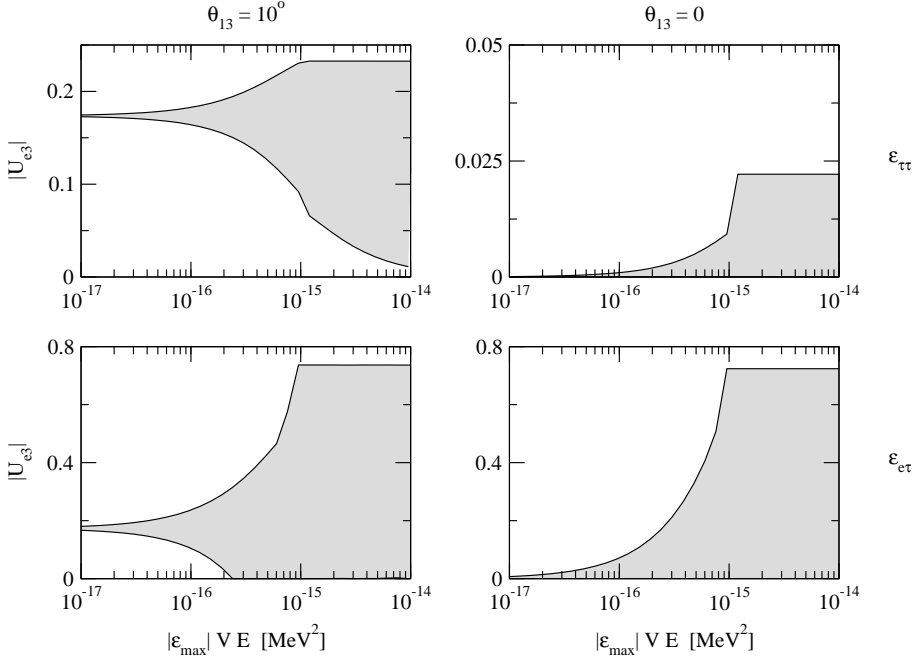


Figure 2: The range of possible $|\tilde{U}_{e3}|$ as a function of $\epsilon_{\max} VE$. The plots are arranged so that the left panels correspond to $\theta_{13} = 10^\circ$ and the right panels to $\theta_{13} = 0$, while the lower panels correspond to a non-standard effect with $\epsilon_{e\tau} \neq 0$ and the upper panels to a non-standard effect with $\epsilon_{\tau\tau} \neq 0$. The qualitative behavior for other values of θ_{13} is similar to the behavior for $\theta = 10^\circ$. (Note the different scales on the vertical axes.)

where we sum over different types of fermions, $\epsilon_{\alpha\beta}^f$ depends on the non-standard interaction with the fermion f , and N_f is the number density of the fermion f . In addition, $\epsilon_{\alpha\beta}^f$ is often split into $\epsilon_{\alpha\beta}^f = \epsilon_{\alpha\beta}^{fL} + \epsilon_{\alpha\beta}^{fR}$, where L and R denotes the projector used in the fermion factor of the effective non-standard Lagrangian density, *i.e.*,

$$\mathcal{L}_{\text{eff}} = -2\sqrt{2}G_F \sum_f \sum_{P=L,R} \epsilon_{\alpha\beta}^{fP} (\bar{\nu}_\alpha \gamma_\rho L \nu_\beta) (\bar{f} \gamma^\rho P f). \quad (33)$$

Recent bounds for $\epsilon_{\alpha\beta}^{fP}$ can be found in Ref. [52] for electron neutrino interactions with electrons (*i.e.*, $\epsilon_{e\beta}^{eP}$) and Ref. [53] for interactions with first generation Standard Model fermions. As an example, the bounds from Ref. [52] for the $\epsilon_{e\tau}$ (which is considered in Fig. 2) are

$$-0.90 < \epsilon_{e\tau}^{eL} < 0.88 \quad \text{and} \quad -0.45 < \epsilon_{e\tau}^{eR} < 0.44, \quad (34)$$

respectively. From Fig. 2, we can deduce that the off-diagonal $\epsilon_{e\tau}$ terms have a larger potential of altering the value of $|\tilde{U}_{e3}|$ than the diagonal $\epsilon_{\tau\tau}$ terms, the maximal value can even exceed $1/\sqrt{2}$, corresponding to $\tilde{\theta}_{13} = 45^\circ$. In addition, it is possible to suppress the effective θ_{13} to zero if introducing non-standard effects. It follows that a relatively large θ_{13} signal, bounded only by the size of the non-standard effects, can be induced or that a large θ_{13} signal can be suppressed by non-standard effects. Note that the effects quickly

disappear at low energies. In order to tell a genuine θ_{13} signal apart from a signal induced by non-standard interactions, it is necessary to study the actual distortion of the energy spectrum induced by the neutrino oscillations.

5 Experimental strategies

Since a general analytic discussion of three-flavor neutrino oscillation including non-standard Hamiltonian effects would be very complicated, we focus on two neutrino flavors in this section. This approach can be justified if one assumes that the other contributions are exactly known, *i.e.*, the neutrino oscillation parameters are measured with sufficient accuracy at some point in the future. Of course, for short-term applications, small non-standard effects might be confused with other small effects such as $\sin^2(2\theta_{13})$ effects [26]. Thus, a comprehensive quantitative discussion would be very complicated at present. In this section, we therefore discuss general strategies to test and identify non-standard effects in long terms based on two-flavor limits.

5.1 Two-flavor limits of neutrino oscillation probabilities

In three-flavor neutrino oscillations, we can construct several interesting two-flavor limits of the probabilities $P_{\alpha\beta}$ including non-standard effects related to two-flavor neutrino oscillations (see, *e.g.*, Ref. [54]):

$$P_{ee} \xrightarrow[\Delta m_{21}^2 \rightarrow 0]{} 1 - \sin^2(2\tilde{\theta}_{13}) \sin^2\left(\frac{\Delta\tilde{m}_{31}^2 L}{4E}\right), \quad (35)$$

$$P_{ee} \xrightarrow[\theta_{13} \rightarrow 0]{} 1 - \sin^2(2\tilde{\theta}_{12}) \sin^2\left(\frac{\Delta\tilde{m}_{21}^2 L}{4E}\right), \quad (36)$$

$$P_{\mu e} \xrightarrow[\Delta m_{21}^2 \rightarrow 0]{} \sin^2(2\tilde{\theta}_{13}) \sin^2\left(\frac{\Delta\tilde{m}_{31}^2 L}{4E}\right) \sin^2(\theta_{23}), \quad (37)$$

$$P_{\mu\mu} \xrightarrow[\Delta m_{21}^2 \rightarrow 0, \theta_{13} \rightarrow 0]{} 1 - \sin^2(2\tilde{\theta}_{23}) \sin^2\left(\frac{\Delta\tilde{m}_{31}^2 L}{4E}\right). \quad (38)$$

Note that all of these probabilities contain the standard matter effects except from $P_{\mu\mu}$. In general, the $su(3)$ generators (the Gell-Mann matrices) will give the degrees of freedom for non-standard Hamiltonian effects with three flavors. However, when studying the effective two-flavor neutrino oscillations, we only use the $su(3)$ generators which are the equivalents of the Pauli matrices in the two-flavor sector that is studied. In addition, one can create two-flavor limits for oscillations into sterile neutrinos.

As stated above, the effective two-flavor neutrino oscillation scenarios should be defined in terms of the effective two-flavor sector in question. For example, in the limit when $\Delta m_{21}^2 \rightarrow 0$, the effective two-flavor sector is spanned by ν_e and $\nu_a = -s_{23}\nu_\mu + c_{23}\nu_\tau$. Thus, the limit can be considered as an exact pure two-flavor scenario only if the non-standard effects preserve the two-flavor limit (*i.e.*, no off-diagonal terms mixing ν_e and ν_a with the remaining neutrino state $\nu_b = c_{23}\nu_\mu + s_{23}\nu_\tau$). If the non-standard addition to the Hamiltonian

is given by

$$H'_{\alpha\beta} = \epsilon_{\alpha\beta} V, \quad (39)$$

then the corresponding addition in the basis spanned by $\{\nu_e, \nu_b, \nu_a\}$ is

$$H' = V \begin{pmatrix} \epsilon_{ee} & c_{23}\epsilon_{e\mu} - s_{23}\epsilon_{e\tau} & c_{23}\epsilon_{e\tau} + s_{23}\epsilon_{e\mu} \\ c_{23}\epsilon_{e\mu}^* - s_{23}\epsilon_{e\tau}^* & A & B \\ c_{23}\epsilon_{e\tau}^* + s_{23}\epsilon_{e\mu}^* & B^* & C \end{pmatrix}, \quad (40)$$

where

$$\begin{aligned} A &= c_{23}^2 \epsilon_{\mu\mu} + s_{23}^2 \epsilon_{\tau\tau} - s_{23} c_{23} (\epsilon_{\mu\tau} + \epsilon_{\mu\tau}^*), \\ B &= c_{23} \epsilon_{\mu\tau} - s_{23}^2 \epsilon_{\mu\tau}^* + s_{23} c_{23} (\epsilon_{\mu\mu} - \epsilon_{\tau\tau}), \\ C &= s_{23}^2 \epsilon_{\mu\mu} + c_{23}^2 \epsilon_{\tau\tau} + s_{23} c_{23} (\epsilon_{\mu\tau} + \epsilon_{\mu\tau}^*). \end{aligned}$$

From this relation, we deduce that the limit will be a pure two-flavor case if $\epsilon_{\alpha\beta} = 0$ for all non-standard effects which do not involve ν_e and $c_{23}\epsilon_{e\mu} - s_{23}\epsilon_{e\tau} = 0$ (which could be implemented by, *e.g.*, $\theta_{23} = 45^\circ$ and $\epsilon_{e\mu} = \epsilon_{e\tau}$).

5.2 Flavor effects for large and small mixing

In this section, we concentrate on pure flavor effects, where we want to understand the limits of very large and very small mixing in view of the probability limits in Eqs. (35)–(38). When the mixing goes to maximal, we have $\cos(2\theta) \rightarrow 0$. This means that the resonance condition in Eq. (17) cannot be fulfilled for $F_3 = 0$ (*i.e.*, “matter resonance”) at reasonably large energies.⁴ From Eq. (15), we can easily observe that F_1 and F_2 will not modify $\sin^2(2\tilde{\theta})$ at all in the absence of matter (and F_3) effects (for example, in $P_{\mu\mu}$ or a vacuum probability). Independent of matter effects, F_3 can increase the suppression of $\sin^2(2\tilde{\theta})$ for large energies. If the resonance condition in Eq. (17) is fulfilled, then $\sin^2(2\tilde{\theta})$ will be independent of F_1 and F_2 . However, in the presence of matter effects (such as for P_{ee} in the limit $\theta_{13} \rightarrow 0$), F_1 and F_2 can reduce the matter effect suppression of $\sin^2(2\tilde{\theta})$ for large energies (*cf.*, Fig. 1), *i.e.*, they can increase the effective mixing. Eventually, it is obvious from Eqs. (14) and (16) that the oscillation frequency is always increased for positive $F_i/\Delta m^2$ ’s.

For small mixing, such as for Eq. (37), we show in Fig. 3 the neutrino oscillation appearance probability $P_{\alpha\beta}$ for two flavors with small mixing, where the effects of the F_i ’s are parameterized relative to the matter effects (*i.e.*, “1” on the vertical axis correspond to an effect with $F_i = V$ and “0” to no non-standard effects). In this figure, many of the following analytic observations are visualized. The resonance condition in Eq. (17) can always be fulfilled for the matter resonance ($F_3 = 0$) by an appropriate choice of energy, baseline, neutrinos or antineutrinos, and oscillation channel. Obviously, we can read off from Eq. (15) that at the resonance $\sin^2(2\tilde{\theta}) \rightarrow 1$, where the matter resonance condition can be influenced by F_3 according to Eq. (17). Therefore, the magnitude of $\sin^2(2\tilde{\theta})$ at the resonance (but not

⁴Note that, in this section, we assume that matter effects determine the resonance energy and the non-standard effects are sub-leading contributions, which may shift the resonance energy. Thus, we refer to the “matter resonance” as the resonance condition in Eq. (17) for $F_3 = 0$.

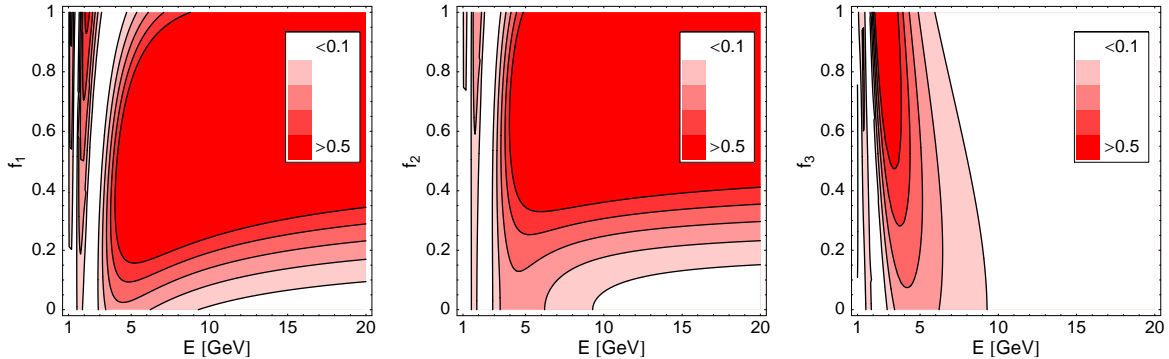


Figure 3: The two-flavor appearance probability $P_{\alpha\beta}$ as a function of energy and the flavor conserving/violating fraction $f_i \equiv F_i/V$ (normalized relative to matter effects). For the values of the neutrino parameters, we have used $\theta = 0.16 \simeq 9.2^\circ$, $\Delta m^2 = 0.0025 \text{ eV}^2$, $L = 3000 \text{ km}$, $\rho = 3.5 \text{ g/cm}^3$, neutrinos only, $\Delta m^2 > 0$, and $f_i > 0$.

necessarily $P_{\alpha\beta}$) is independent of F_1 , F_2 , and F_3 . However, F_3 can shift the position of the resonance (such as in energy space). If we choose an energy far above the resonance energy and $F_i/V \ll 1$ ($i = 1, 2, 3$), then we have

$$\sin^2(2\tilde{\theta}) \rightarrow \frac{\left[\frac{4EF_1}{\Delta m^2} + \sin(2\theta)\right]^2 + \left(\frac{4EF_2}{\Delta m^2}\right)^2}{\left[\frac{2VE}{\Delta m^2} + \frac{4EF_3}{\Delta m^2} - 1\right]^2}. \quad (41)$$

This means that F_1 and F_2 can for large enough energies enhance a flavor transition, *i.e.*, they increase the oscillation amplitude. In addition, for positive $F_1/\Delta m^2$, one can observe from this equation that an enhancement effect of F_1 is always larger than the F_2 effect of the same size, since F_1 is also enhanced by the mixed term $8EF_1 \sin(2\theta)/\Delta m^2$ in the numerator compared with the contribution from F_2 . In principle, one could distinguish F_1 from F_2 by a measurement at two different energies, because the mixed term has a linear (instead of quadratic) energy dependence. In practice, such a discrimination should be very hard. In addition, the quantity F_3 can play the same role as the matter potential V , *i.e.*, it can reduce the flavor transition for large energies. However, note that one can construct cancellations between the matter potential V and F_3 leading to conditions similar to the ones which follow from Eq. (18). From Eqs. (14) and (16), we can read off that even for positive F_i 's the oscillation frequency can be reduced for F_3 if we measure below the matter resonance. Therefore, given specific non-standard effects determining at least the signs of Eq. (18), a measurement below the resonance might help to identify F_1 and F_2 versus F_3 already by the sign of the Δm_{31}^2 change (for positive V).

5.3 Mass effects and other non-standard possibilities

In Sec. 3.3, we have discussed mass effects, such as coming from MVN. Since a pure M_1 or M_3 effect, translates into a combination of F_1 and F_3 [*cf.*, Eq. (13)], we expect to find a mixture of F_1 and F_3 effects, *i.e.*, both F_1 and F_3 effects have to be present. Thus, if we assume that there is only one dominating “pure” non-standard contribution (F_1 , F_2 , F_3 ,

M_1 , M_2 , or M_3), then this simultaneous presence points towards a mass effect. Clearly, an M_2 effect, on the other hand, cannot be distinguished from an F_2 effect. A different property of M_3 is not so obvious from Sec. 3.3, but very obvious already from Eqs. (1), (2), and (6): Since M_3 enters diagonal in mass basis, it corresponds to an energy dependent shift of the vacuum mass squared difference. As a consequence, in vacuum, the effective mixing angle is not modified by M_3 [*cf.*, Eq. (22)]. Thus, the oscillation amplitudes are not modified by M_3 , but the oscillation pattern shifts (contrary to F_3 effects, where also the amplitude changes). In this case, the resonance condition becomes meaningless and the amplitude becomes $\sin^2(2\tilde{\theta}) = \sin^2(2\theta)$.

Another class of effects has been discussed by Blennow *et al.* in Ref. [1]. In this study, so-called “damping effects” could describe modifications on probability level instead of Hamiltonian level (such as neutrino decay, absorption, wave packet decoherence, oscillations into sterile neutrinos, quantum decoherence, averaging, *etc.*). It is obvious from Eq. (3) in Ref. [1] that these damping effects do not alter the oscillation frequency. However, the oscillation amplitude can be damped either by a damping of the overall probability (“decay-like damping”) or by the oscillating terms only (“decoherence-like damping”). In the first case, the total probability of finding a neutrino in any neutrino state is damped for all energies, whereas in the second case, it is constantly equal to one while the individual neutrino oscillation probabilities are damped in the oscillation maxima and enhanced in the oscillation minima.

Since all (small) effects one could imagine in quantum field theory, involving the modification of fundamental interactions or propagations, can be described by either coherent or incoherent addition of amplitudes, one can expect that the two classes of Hamiltonian and probability (damping) effects can cover all possible effects. However, in practice, potential energy, environment, and explicit time dependencies (such as from a matter potential) can make life more complicated. In the next section, we therefore describe some general qualitative strategies how to identify particular classes of effects.

5.4 Where can one look for non-standard effects?

In order to identify non-standard effects quantitatively, one will in any realistic experiment have to fit the energy spectrum and marginalize over the (standard) neutrino oscillation parameters. However, we discuss qualitative changes of the observables in this section, where we refer to observables ($P_{\alpha\beta}$, $\sin^2(2\theta)$, Δm^2 , *etc.*) modified by non-standard effects in addition to standard neutrino oscillations. Note that mass squared differences and mixing angles are not directly observable and require the information at different L/E ’s. For instance, a shift in the neutrino oscillation probability is not detectable by the measurement at one L/E . However, dividing the energy range into two sub-ranges and finding two significantly different oscillation frequencies points towards a shift of the oscillation frequency as function of energy. In the following, we therefore imply that we use all available spectral (energy) information.

As is obvious from Eqs. (14) and (16), it is a general feature of non-standard Hamiltonian effects that the oscillation frequency is changed. Therefore, in order to investigate such effects, one would like to measure the spectral distortion by the oscillation frequency as

good as possible. This also implies that one can hardly search for general non-standard Hamiltonian effects smaller than the precision of the oscillation frequency. However, in specific cases, the spectral (energy) dependence of an effect may help (which we do not discuss any further). If one identifies such a frequency irregularity, then it is a good option to choose a channel with a matter resonance. Fitting the whole spectrum around the resonance, any shift of the resonance energy points towards an F_3 effect. It is obvious from Eqs. (15) and (16) that the critical quantity F_3 is directly correlated with the matter potential V , *i.e.*, one cannot establish effects more precisely than the matter density uncertainty. In addition, a measurement at large energies can reveal if the matter effect suppression is reduced which would point towards an F_1 and F_2 effect. Of course, such a flavor violating effect could easily be confused with a different mixing angle θ , which means that the mixing angle has to be very well known or that one has information from many different energies. The discrimination between F_1 and F_2 requires excellent spectral information and a high-precision determination of the mixing angle, which means that it should be rather hard to discriminate F_1 and F_2 , at least for small mixing.

If two effects (F_1 and F_3) are detected simultaneously, then it is likely that we deal with a mass effect (M_1 or M_3). However, in order to uniquely determine at least an M_1 effect, the precise combination of F_1 , F_3 , and θ has to be known [*cf.*, Eq. (13)]. Therefore, such a direct test makes it hard to identify mass effects uniquely, and thus, other indirect methods might be preferable (such as modified MSW transitions in the Sun [30, 31]). An M_3 effect, on the other hand, corresponds to an energy-dependent shift of the intrinsic vacuum neutrino oscillation probabilities. Therefore, extracting Δm^2 in two different energy ranges without any change of the vacuum mixing angle could reveal this effect. As we have discussed, an M_2 effect can, by definition, not be distinguished from an F_2 effect.

If a spectrum covering more than one oscillation maximum reveals that the positions of the oscillation nodes correspond to standard neutrino oscillations, but the oscillation amplitudes are modified, then it is likely that we are dealing with a damping effect. A reduction of the total event rate (summed over all bins) points towards a “decay-like” damping effect, whereas the conservation of the total event rate and an enhancement of the oscillation minimum points towards a “decoherence-like” damping. In order to establish a damping effect, it is therefore very important to measure the oscillation nodes precisely and to know the signal normalization very well.

For a damping effect, the energy signature could reveal the actual nature of the effect [1], whereas for a Hamiltonian effect, the correlations with the oscillation frequencies should make this determination much harder. However, small energy dependencies within the analysis range should qualitatively not change the results as long as the F_i rises stronger than E^{-1} . For explicitly time-dependent systems, the results only hold within regions of small time dependencies. In Table 1, we summarize our qualitative approaches to test non-standard effects.

Type of test	Hamiltonian effects						“Damping” effects	
	F_1	F_2	F_3	M_1	M_2	M_3	“Decay-like”	“Decoh.-like”
Osc. frequency changed?	Y	Y	Y	Y	Y	Y	N	N
Ampl. at high E enhanced?	Y	Y	N	Y	Y	Y	n/a	n/a
Matter resonance shifted?	N	N	Y	Y	N	Y	n/a	n/a
Peak amplitudes unchanged?	N	N	N	N	N	Y	N	N
Compare diff. E ’s	D	D		n/a			n/a	
Osc. minima enhanced?				n/a			N	Y
Total rate reduced?				n/a			Y	N

Table 1: Different principle tests for non-standard effects. “Y” (Yes) and “N” (No) refer to a possible identifier for an effect (for appropriate parameters), “D” to a potential discriminator between two effects, and “n/a” to “not applicable”. See main text for more details.

6 A numerical example: Neutrino factory for large $\sin^2(2\theta_{13})$

This section is not supposed to be a complete study of non-standard Hamiltonian effects, but to demonstrate some of the qualitatively discussed properties from the last sections in a complete numerical simulation of a possible future experiment. Therefore, we have to make a number of assumptions. We use a modified version of the GLoBES software [56] to include non-standard effects. As a future high-precision instrument, we choose the neutrino factory experiment setup from Ref. [57, 58] with $L = 3\,000$ km, a 50 kt magnetized iron calorimeter detector, $1.06 \cdot 10^{21}$ useful muon decays per year, and four years of running time in each polarity.⁵ For the neutrino oscillation parameters, we use $\sin^2 2\theta_{12} = 0.83$, $\sin^2 2\theta_{23} = 1$, $\Delta m_{21}^2 = 8.2 \cdot 10^{-5}$ eV², and $\Delta m_{31}^2 = 2.5 \cdot 10^{-3}$ eV² [51, 59–61], as well as we assume a 5% external measurement for Δm_{21}^2 and θ_{12} [60] and include matter density uncertainties of the order of 5% [62, 63]. In order to test precision measurements of the non-standard effects, we use $\sin^2(2\theta_{13}) = 0.1$ close to the CHOOZ bound [64], as well as we assume a normal mass hierarchy and $\delta_{\text{CP}} = 0$. For simplicity, we do not take the $\text{sgn}(\Delta m_{31}^2)$ -degeneracy [65] into account, but we include the intrinsic $(\theta_{13}, \delta_{\text{CP}})$ -degeneracy [66], whereas the octant degeneracy does not appear for maximal mixing [67]. Note that we do *not* include external bounds on the non-standard physics and $\sin^2(2\theta_{13})$, which, for instance, mean that we allow “fake” solutions of $\sin^2(2\theta_{13})$ above the upper bound. This assumption is plausible, since, depending on the effect, the CHOOZ bound may have been affected by the non-standard effect as well.

Since we choose $\sin^2(2\theta_{13})$ to be large, let us focus on the appearance channel of ν_e oscillating into ν_μ (or $\bar{\nu}_e$ oscillating into $\bar{\nu}_\mu$). Expanded in small $\sin^2(2\theta_{13})$ and $\alpha \equiv \Delta m_{21}^2 / \Delta m_{31}^2$, we have for $\alpha \rightarrow 0$ (which should be a good approximation for $\sin^2(2\theta_{13}) \gg \alpha^2 \simeq 0.001$) [68–70]

$$P_{e\mu} \sim \sin^2 2\theta_{13} \sin^2 \theta_{23} \frac{\sin^2[(1 - \hat{A})\Delta]}{(1 - \hat{A})^2}, \quad (42)$$

⁵Compared to Ref. [57], we use a 2.5% systematic normalization error for all channels as in Ref. [58].

where $\Delta \equiv \Delta m_{31}^2 L / (4E)$ and $\hat{A} \equiv \pm 2\sqrt{2}G_F n_e E / \Delta m_{31}^2$. This means that we are effectively dealing with the two-flavor limit described in Sec. 5.1. Using the parameterization in Eqs. (4) and (5) applied to the 1-3-sector, we therefore adopt the following Hamiltonian:

$$\begin{aligned} H = & \frac{1}{2E} U \begin{pmatrix} M_3 & 0 & M_1 - iM_2 \\ 0 & \Delta m_{21}^2 & 0 \\ M_1 + iM_2 & 0 & \Delta m_{31}^2 - M_3 \end{pmatrix} U^\dagger \\ & + \begin{pmatrix} V + F_3 & 0 & F_1 - iF_2 \\ 0 & 0 & 0 \\ F_1 + iF_2 & 0 & -F_3 \end{pmatrix}. \end{aligned} \quad (43)$$

Note that this parameterization does not exactly correspond to the two-flavor limit even for $\alpha \rightarrow 0$, since there are some non-trivial mixing effects in the 2-3-sector as stated in Sec. 5.1. However, we will demonstrate some of the characteristics from Sec. 5 with this approach. In addition, note that we have now adopted a specific energy dependence of the mass and flavor effects. In this case, the mass effects correspond to MVNs changing the mass eigenstates, whereas the flavor effects correspond to some non-standard interactions approximately constant in energy. Eventually, we will quantify the size of the F_i and M_i in terms of $f_i = F_i/V$ (for $\rho = 3.5 \text{ g/cm}^3$) and $\mu_i = M_i/\Delta m_{31}^2$ (for $\Delta m_{31}^2 = 2.5 \cdot 10^{-3} \text{ eV}^2$). This quantification makes sense, since it is obvious from Eq. (43) that the effect of these quantities will have to be compared with the order of V and Δm_{31}^2 , respectively. In addition, note that $f_1 - i f_2 = \epsilon_{e\tau}^e$ from Sec. 4, which means that it will be interesting to compare the precisions of f_1 and f_2 to the current bounds for $\epsilon_{e\tau}$.

As a first analysis, we show in Fig. 4 the correlation between simulated and fit pure effects. Therefore, we simulate a pure effect (column) and fit it with a different one (row), *i.e.*, we marginalize over the respective f_i or μ_i . The areas of the disks are proportional to the minimum simulated value necessary to establish a 3σ effect, where we have chosen a cutoff of $|f_i| \lesssim 0.3$ and $|\mu_i| \lesssim 0.5$ (corresponding to largest gray disks).⁶ This means that the size of the disks measures the correlation between two pure effects and the ability to discriminate those. One can easily make a number of qualitative observations from Sec. 5 quantitative. First, it is hard to discriminate between F_1 and F_2 , since these effects are qualitatively similar and highly correlated with θ_{13} (as we have tested). However, if Nature implemented a flavor-changing F_1 or F_2 effect, then one could easily establish it against F_3 and the pure mass effects. In general, note that a discrimination between flavor and mass effects is rather easy because of their different spectral dependence in this example (such as between F_2 and M_2). The difference to F_3 can be explained by the different flavor-conserving nature of F_3 . The results look somewhat different for the F_3 column: Because of the correlation with ρ and all of the neutrino oscillation parameters (see below), it will be hard to establish this effect. For the simulated mass effects, the scale is different, *i.e.*, one cannot directly compare the M -columns with the F -columns. Again, the mass effects can be distinguished from the flavor effects rather easily. However, it is quite impossible to establish a mass effect against another one. For M_1 and M_2 , the reason is correlations with mainly all of the mixing angles, since one could think about a re-diagonalization of the mass matrix being absorbed

⁶Note that, for instance, the gray disks for f_1 and f_2 correspond to the order of magnitude of the upper bounds in Eq. (34), which means that testing considerably larger effects does not make sense.

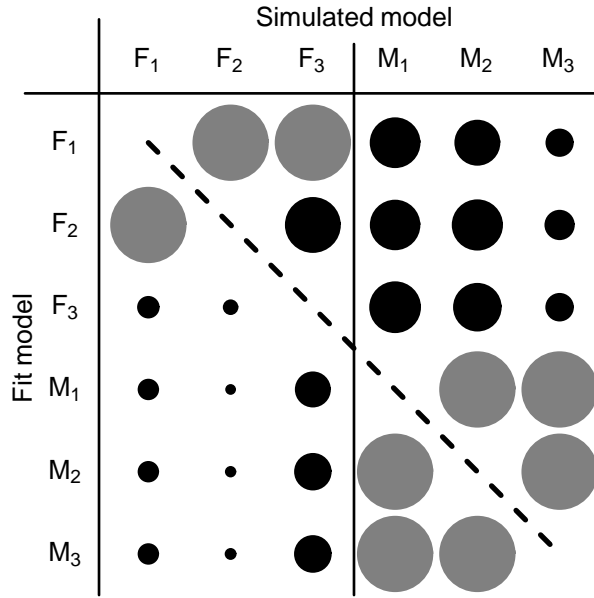


Figure 4: Correlation between simulated models (columns) and fit models (rows). The areas of the disks represent the discovery potentials of the simulated “pure” effects (parameterized in terms of f_i or μ_i) given that a different pure effect (fit model) is allowed (minimum value of a deviation from zero necessary in either direction for a 3σ discovery). Therefore, the larger the disk, the more difficult it will be to distinguish a pure effect from another one. Note that we use cutoffs of $|f_i| \lesssim 0.3$ and $|\mu_i| \lesssim 0.5$ (largest gray disks), since some models cannot even be distinguished for much larger values. The areas of the rest of the disks are normalized with respect to these cutoffs for simulated flavor and mass effects.

by the mixing matrix. However, for M_3 , we find an extreme correlation with Δm_{31}^2 . This is expected, since M_3 effectively changes Δm_{31}^2 .

In Fig. 5, we show the impact factors for the test of specific simulated models against standard three-flavor neutrino oscillations. Again, a number of aspects from Sec. 5 can be verified. For F_1 and F_2 effects, systematics is the main impact factor, since these flavor effects determine the overall height of the appearance signal and are not introduced with a specific spectral dependence (remember that we use a conservative overall normalization error of 2.5%). For F_3 effects, we have earlier determined the matter density uncertainty as an important constraint. However, improving the knowledge on δ_{CP} , θ_{13} , or Δm_{31}^2 does have a similar effect, since the extraction of the individual parameters becomes easier. For the mass effects, we encounter a completely different behavior. Remember that we have defined the mass effects with the same energy dependence as the mass squared differences, which means that particularly M_3 is easily mixed up with Δm_{31}^2 . On the other hand, M_1 and M_2 are related to a flavor change in the appearance channel via the mixing matrix, *i.e.*, θ_{13} . Therefore, it is not surprising that such a flavor change can be interpreted either as mixing or mass-changing effect. Compared to Sec. 5, there are also a number of differences coming from the three-flavor treatment (solar and CP -effects) and the mixing in the 2-3-sector. These effects introduce additional correlations with δ_{CP} and θ_{23} . However, they are

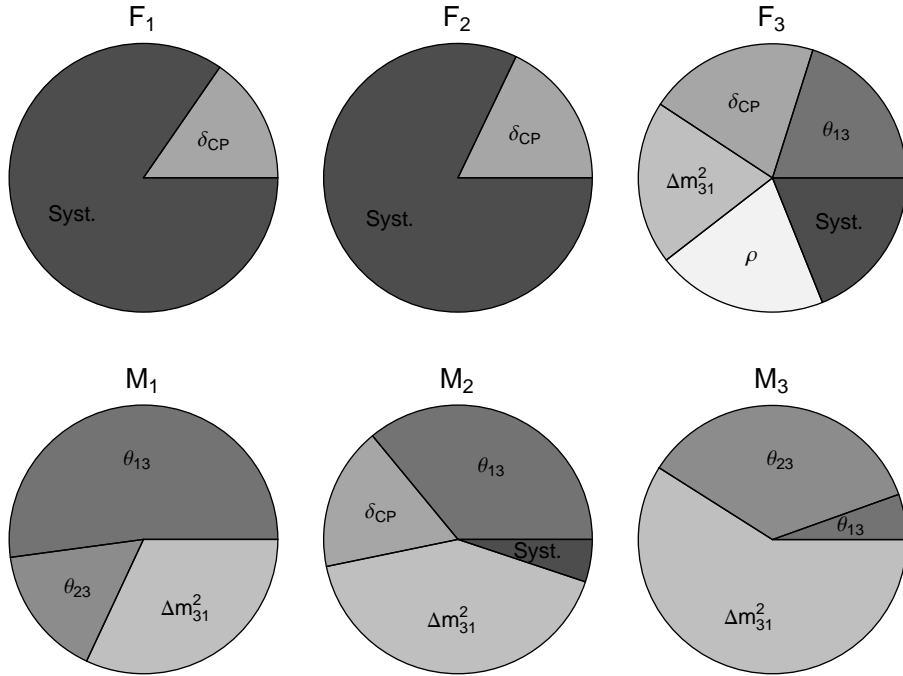


Figure 5: Main impact factors (impact $> 5\%$) for the test of specific simulated models (captions) against standard three-flavor neutrino oscillations (3σ measurement). The neutrino oscillation parameters refer to correlations with the respective parameter, “Syst.” refers to systematics, and “ ρ ” refers to the matter density uncertainty. The impact factors are defined as in Ref. [57] as relative improvement when the respective quantity is fixed (correlations) or systematics is switched off.

also the reason that M_3 can be constrained at all from this experiment alone [in the pure two-flavor case, it would be impossible to distinguish between a non-vanishing M_3 and a different Δm_{31}^2 if the mass effects have the energy dependence assumed in Eq. (43)].

Finally, in Table 2, we show the discovery reaches for the parameters from Eq. (43) against the standard three-flavor neutrino oscillation scenario. Comparing the precisions of f_1 and f_2 with the numbers in Eq. (34) is impressive. However, these discovery reaches depend on $\sin^2(2\theta_{13})$ (and δ_{CP}) and we have assumed a very large $\sin^2(2\theta_{13}) = 0.1$ (and $\delta_{CP} = 0$). Note that the reach in f_2 is actually better than the one for f_1 , which is different from what is found in the two-flavor limit in Sec. 5. The reasons are the mixing effects in the 2-3-sector and that F_2 is a non-trivial source of CP -violation in the three-flavor case.

7 Summary and conclusions

In summary, we have studied non-standard effects on neutrino oscillations on Hamiltonian level. We have parameterized these effects in terms of the generators of Lie algebras. In particular, we have derived effective parameter mappings in the two-flavor limit. Although

Quantity	Lower limit (1σ)	Upper limit (1σ)	Lower limit (3σ)	Upper limit (3σ)
f_1	−0.008	0.008	−0.025	0.026
f_2	−0.003	0.003	−0.008	0.008
f_3	−0.016	0.016	−0.049	0.082
μ_1	−0.176	0.118	−0.218	0.211
μ_2	−0.105	0.126	−0.181	0.212
μ_3	−0.015	0.015	−0.044	0.090

Table 2: Discovery limits for the parameters in Eq. (43) as parameterized $f_i = F_i/V$ and $\mu_i = M_i/\Delta m_{31}^2$ from the neutrino factory simulation (including correlations).

these mappings can only be used for two neutrino flavors, they allow the discussion of arbitrarily large non-standard effects and the change of the corresponding resonance conditions. Furthermore, we have visualized the effects and discussed their properties. Eventually, we have discussed experimental strategies how one, in principle, could test small contributions of such effects, where we have used two-flavor limits of three-flavor neutrino oscillation probabilities for illustration.

In the literature, there are different classes of non-standard Hamiltonian effects, which are effects in flavor basis (such as FCNC and NSI) and in mass basis (such as MVN). As a trivial fact, we have demonstrated that there is, in principle, no mathematical difference between these effects if one allows the most general form in each base, *i.e.*, they can be described as superpositions of each other [*cf.*, Eq. (13)]. Given the detection of a general non-standard effect on Hamiltonian level, it is therefore not possible to classify it as a flavor or mass effect without further assumptions or knowledge and, from an empirical point of view, the classification is a matter of definition. Therefore, we have defined “pure” effects as effects which are proportional to individual generators. Those correspond to pure flavor/mass conserving/violating effects, *i.e.*, effects which affect particular flavor or mass eigenstates. It is then the simplicity of the form in their respective basis which defines them to be flavor or mass effects. The reason to introduce the concept of pure effects is that they correspond to phenomenologically different interpretations, such as FCNC, NSI, or MVN, and specific models usually have patterns which are as simple as possible in the respective bases. Therefore, the concept of these pure effects allows the choice of the most “natural” class of models for further testing, which is most appealing from the physics point of view.

From the two-flavor mappings of the neutrino oscillation parameters, we have derived the modified mass squared differences and mixing angles for pure effects as well as the modified resonance conditions including standard matter effects. In flavor basis, we have found that while any flavor violating pure effect can obviously change the transition probabilities, it does not affect the resonance condition. In addition, it does not change the mixing angle at the resonance itself. However, a flavor conserving pure effect changes the resonance condition similar to matter effects. In addition, it can suppress the flavor transition for large energies similar to matter effects even in vacuum. Pure mass effects behave, in principle, as rotations of the flavor effects by the mixing angles, *i.e.*, a pure mass effect will be observed as a linear combination of flavor effects. However, for a pure mass conserving effect, these flavor effects combine with special characteristics, since the mass effect is similar to an (energy dependent)

change of the vacuum mass squared difference, *i.e.*, it basically squeezes or stretches the oscillation pattern.

We have also studied some aspects of the three-flavor generalization of general non-standard Hamiltonian effects using perturbation theory as well as numeric calculations. By assuming small non-standard Hamiltonian effects, we have derived expressions for the effective matrix elements using perturbation theory and observed how the confusion theorem between θ_{13} and non-standard effects described in Ref. [26] arises at the Hamiltonian level. The numeric calculations show that non-standard interactions can alter the determination of θ_{13} significantly at higher energies, while still preserving a high accuracy at lower energies (*cf.*, Fig. 2).

Given the described calculations, we have studied possible experimental strategies to find non-standard effects using two-flavor limits of the three-flavor neutrino oscillation probabilities and the limits of small and very large mixing for illustration. Since in quantum field theory any non-standard effect may originate in the coherent (Hamiltonian effect) or incoherent (“damping” effect) summation of amplitudes, we have compared the non-standard Hamiltonian effects to the previously studied “damping” effects on probability level. We have found that these two classes can be distinguished by typical characteristics. Non-standard Hamiltonian effects shift the oscillation pattern, while “damping” effects, in general, do not. The different classes of non-standard Hamiltonian effects can, in principle, be identified by their modification of oscillation amplitudes for large energies, the shift of the matter resonance, the comparison of different L/E -ranges, *etc.*, where we have developed a classification table for these qualitative identifiers. We have also discussed the bottlenecks to these approaches, such as the matter density uncertainty preventing the determination of pure flavor conserving effects beyond the precision to which the matter density is known.

Eventually, we have demonstrated, at a numerical example for a neutrino factory, that many of these features can be found in a realistic experiment simulation using three flavors and specific spectral (energy) dependencies of the non-standard effects. For example, while it is simple to distinguish a flavor-changing from flavor-conserving or mass effects in general, mass effects are hard to establish as long as the oscillation parameters are not precisely known (because they could be rotated away). In addition, we have compared the obtainable discovery reaches for $\epsilon_{e\tau}$ to the current limits, and we have found at least an order of magnitude improvement for large $\sin^2(2\theta_{13})$ and $\delta_{\text{CP}} = 0$.

Since the past has told us that neutrinos are good for surprises, the high precision of future neutrino oscillation experiments might as well reveal a detection of “new physics” beyond the Standard Model (extended to include massive neutrinos). Therefore, we conclude that one should include general strategies to look for non-standard effects in future neutrino oscillation experiments, where we have followed a “top-down” approach: Instead of testing particular models (“bottom-up”), we have assumed that some inconsistency will be found first. Secondly, one may want to classify this inconsistency to be either a Hamiltonian or a probability level (“damping”) effect. Finally, individual models are identified which fit this effect. Since we do not know exactly what we are looking for, such an approach might be a clever search strategy. Future studies should demonstrate how such an approach can be most efficiently extended to three neutrino flavors, which oscillation channels are most suitable, and what the correlations with the existing fundamental neutrino oscillation

parameters imply.

Acknowledgments

W.W. would like to thank the Theoretical Elementary Particle Physics group at KTH for the warm hospitality during a research visit. In addition, T.O. and W.W. would like to thank Manfred Lindner and his group at TUM in Munich for the warm hospitality during their research visits where parts of this paper were developed.

This work was supported by the Royal Swedish Academy of Sciences (KVA), the Swedish Research Council (Vetenskapsrådet), Contract Nos. 621-2001-1611, 621-2002-3577, the Göran Gustafsson Foundation, the Magnus Bergvall Foundation, the W. M. Keck Foundation, and NSF grant PHY-0070928.

References

- [1] M. Blennow, T. Ohlsson, and W. Winter, JHEP **06**, 049 (2005), [hep-ph/0502147](#).
- [2] J. W. F. Valle, Phys. Lett. **B199**, 432 (1987).
- [3] J. W. F. Valle, J. Phys. **G29**, 1819 (2003), and references therein.
- [4] S. Bergmann, Nucl. Phys. **B515**, 363 (1998), [hep-ph/9707398](#).
- [5] S. Bergmann and A. Kagan, Nucl. Phys. **B538**, 368 (1999), [hep-ph/9803305](#).
- [6] S. Bergmann, Y. Grossman, and E. Nardi, Phys. Rev. **D60**, 093008 (1999), [hep-ph/9903517](#).
- [7] L. Wolfenstein, Phys. Rev. **D17**, 2369 (1978).
- [8] P. I. Krastev and J. N. Bahcall (1997), [hep-ph/9703267](#).
- [9] S. Bergmann, M. M. Guzzo, P. C. de Holanda, P. I. Krastev, and H. Nunokawa, Phys. Rev. **D62**, 073001 (2000), [hep-ph/0004049](#).
- [10] M. Guzzo *et al.*, Nucl. Phys. **B629**, 479 (2002), [hep-ph/0112310](#).
- [11] A. Friedland, C. Lunardini, and C. Peña-Garay, Phys. Lett. **B594**, 347 (2004), [hep-ph/0402266](#).
- [12] O. G. Miranda, M. A. Tórtola, and J. W. F. Valle (2004), [hep-ph/0406280](#).
- [13] S. Bergmann, Y. Grossman, and D. M. Pierce, Phys. Rev. **D61**, 053005 (2000), [hep-ph/9909390](#).
- [14] N. Fornengo, M. Maltoni, R. Tomàs Bayo, and J. W. F. Valle, Phys. Rev. **D65**, 013010 (2002), [hep-ph/0108043](#).

- [15] M. C. Gonzalez-Garcia and M. Maltoni, Phys. Rev. **D70**, 033010 (2004), [hep-ph/0404085](#).
- [16] A. Friedland, C. Lunardini, and M. Maltoni, Phys. Rev. **D70**, 111301 (2004), [hep-ph/0408264](#).
- [17] A. Friedland and C. Lunardini (2005), [hep-ph/0506143](#).
- [18] G. L. Fogli, E. Lisi, A. Mirizzi, and D. Montanino, Phys. Rev. **D66**, 013009 (2002), [hep-ph/0202269](#).
- [19] B. Bekman, J. Gluza, J. Holeczek, J. Syska, and M. Zrałek, Phys. Rev. **D66**, 093004 (2002), [hep-ph/0207015](#).
- [20] S. Bergmann and Y. Grossman, Phys. Rev. **D59**, 093005 (1999), [hep-ph/9809524](#).
- [21] T. Ota and J. Sato, Phys. Lett. **B545**, 367 (2002), [hep-ph/0202145](#).
- [22] T. Ota, J. Sato, and N.-A. Yamashita, Phys. Rev. **D65**, 093015 (2002), [hep-ph/0112329](#).
- [23] M. C. Gonzalez-Garcia, Y. Grossman, A. Gusso, and Y. Nir, Phys. Rev. **D64**, 096006 (2001), [hep-ph/0105159](#).
- [24] P. Huber and J. W. F. Valle, Phys. Lett. **B523**, 151 (2001), [hep-ph/0108193](#).
- [25] P. Huber, T. Schwetz, and J. W. F. Valle, Phys. Rev. Lett. **88**, 101804 (2002), [hep-ph/0111224](#).
- [26] P. Huber, T. Schwetz, and J. W. F. Valle, Phys. Rev. **D66**, 013006 (2002), [hep-ph/0202048](#).
- [27] M. Campanelli and A. Romanino, Phys. Rev. **D66**, 113001 (2002), [hep-ph/0207350](#).
- [28] P. Gu, X. Wang, and X. Zhang, Phys. Rev. **D68**, 087301 (2003), [hep-ph/0307148](#).
- [29] R. Fardon, A. E. Nelson, and N. Weiner, JCAP **0410**, 005 (2004), [astro-ph/0309800](#).
- [30] V. Barger, P. Huber, and D. Marfatia (2005), [hep-ph/0502196](#).
- [31] M. Cirelli, M. C. Gonzalez-Garcia, and C. Peña-Garay, Nucl. Phys. **B719**, 219 (2005), [hep-ph/0503028](#).
- [32] X.-J. Bi, P.-h. Gu, X.-l. Wang, and X.-m. Zhang, Phys. Rev. **D69**, 113007 (2004), [hep-ph/0311022](#).
- [33] P. Q. Hung and H. Päs, Mod. Phys. Lett. **A20**, 1209 (2005), [astro-ph/0311131](#).
- [34] D. B. Kaplan, A. E. Nelson, and N. Weiner, Phys. Rev. Lett. **93**, 091801 (2004), [hep-ph/0401099](#).
- [35] P.-h. Gu and X.-j. Bi, Phys. Rev. **D70**, 063511 (2004), [hep-ph/0405092](#).

- [36] K. M. Zurek, JHEP **10**, 058 (2004), [hep-ph/0405141](#).
- [37] R. D. Peccei, Phys. Rev. **D71**, 023527 (2005), [hep-ph/0411137](#).
- [38] H. Li, Z.-g. Dai, and X.-m. Zhang, Phys. Rev. **D71**, 113003 (2005), [hep-ph/0411228](#).
- [39] X.-J. Bi, B. Feng, H. Li, and X.-m. Zhang (2004), [hep-ph/0412002](#).
- [40] R. Horvat (2005), [astro-ph/0505507](#).
- [41] N. Afshordi, M. Zaldarriaga, and K. Kohri (2005), [astro-ph/0506663](#).
- [42] R. Takahashi and M. Tanimoto (2005), [hep-ph/0507142](#).
- [43] R. Fardon, A. E. Nelson, and N. Weiner (2005), [hep-ph/0507235](#).
- [44] M. Kawasaki, H. Murayama, and T. Yanagida, Mod. Phys. Lett. **A7**, 563 (1992).
- [45] G. J. Stephenson Jr., T. Goldman, and B. H. J. McKellar, Int. J. Mod. Phys. **A13**, 2765 (1998), [hep-ph/9603392](#).
- [46] G. J. Stephenson Jr., T. Goldman, and B. H. J. McKellar, Mod. Phys. Lett. **A12**, 2391 (1997), [hep-ph/9610317](#).
- [47] R. F. Sawyer, Phys. Lett. **B448**, 174 (1999), [hep-ph/9809348](#).
- [48] C. W. Kim and A. Pevsner Chur, Switzerland: Harwood (1993) 429 p. (Contemporary concepts in physics, 8).
- [49] S. P. Mikheyev and A. Y. Smirnov, Sov. J. Nucl. Phys. **42**, 913 (1985).
- [50] S. P. Mikheyev and A. Y. Smirnov, Nuovo Cim. **C9**, 17 (1986).
- [51] M. Maltoni, T. Schwetz, M. A. Tórtola, and J. W. F. Valle, New J. Phys. **6**, 122 (2004), [hep-ph/0405172](#).
- [52] J. Barranco, O. G. Miranda, C. A. Moura, and J. W. F. Valle (2005), [hep-ph/0512195](#).
- [53] S. Davidson, C. Peña-Garay, N. Rius, and A. Santamaria, JHEP **03**, 011 (2003), [hep-ph/0302093](#).
- [54] E. K. Akhmedov, R. Johansson, M. Lindner, T. Ohlsson, and T. Schwetz, JHEP **04**, 078 (2004), [hep-ph/0402175](#).
- [55] H. Päs, S. Pakvasa, and T. J. Weiler (2005), [hep-ph/0504096](#).
- [56] P. Huber, M. Lindner, and W. Winter, Comput. Phys. Commun. **167**, 195 (2005), [hep-ph/0407333](#).
- [57] P. Huber, M. Lindner, and W. Winter, Nucl. Phys. **B645**, 3 (2002), [hep-ph/0204352](#).
- [58] P. Huber, M. Lindner, M. Rolinec, and W. Winter, Phys. Rev. **D73**, 053002 (2006), [hep-ph/0506237](#).

- [59] G. L. Fogli, E. Lisi, A. Marrone, and D. Montanino, Phys. Rev. **D67**, 093006 (2003), [hep-ph/0303064](#).
- [60] J. N. Bahcall, M. C. Gonzalez-Garcia, and C. Peña-Garay, JHEP **08**, 016 (2004), [hep-ph/0406294](#).
- [61] A. Bandyopadhyay, S. Choubey, S. Goswami, S. T. Petcov, and D. P. Roy (2004), [hep-ph/0406328](#).
- [62] R. J. Geller and T. Hara, Phys. Rev. Lett. **49**, 98 (2001), [hep-ph/0111342](#).
- [63] T. Ohlsson and W. Winter, Phys. Rev. **D68**, 073007 (2003), [hep-ph/0307178](#).
- [64] M. Apollonio *et al.* (CHOOZ), Phys. Lett. **B466**, 415 (1999), [hep-ex/9907037](#).
- [65] H. Minakata and H. Nunokawa, JHEP **10**, 001 (2001), [hep-ph/0108085](#).
- [66] J. Burguet-Castell, M. B. Gavela, J. J. Gomez-Cadenas, P. Hernandez, and O. Mena, Nucl. Phys. **B608**, 301 (2001), [hep-ph/0103258](#).
- [67] G. L. Fogli and E. Lisi, Phys. Rev. **D54**, 3667 (1996), [hep-ph/9604415](#).
- [68] A. Cervera *et al.*, Nucl. Phys. **B579**, 17 (2000), [hep-ph/0002108](#).
- [69] M. Freund, P. Huber, and M. Lindner, Nucl. Phys. **B585**, 105 (2000), [hep-ph/0004085](#).
- [70] M. Freund, Phys. Rev. **D64**, 053003 (2001), [hep-ph/0103300](#).